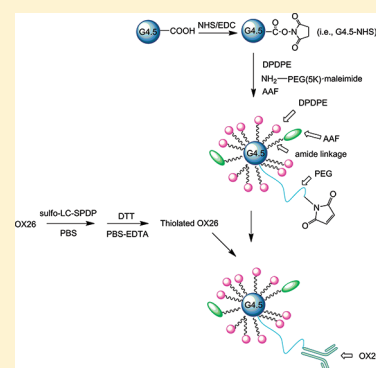


Transbuccal Delivery of CNS Therapeutic Nanoparticles: Synthesis, Characterization, and In Vitro Permeation Studies

Quan Yuan,[†] Yao Fu,[‡] Weiyuan John Kao,^{‡,§} Damir Janigro,^{||,⊥} and Hu Yang^{*,†,‡,¶}[†]Department of Biomedical Engineering, Virginia Commonwealth University, Richmond, Virginia 23284, United States[‡]School of Pharmacy and [§]Department of Biomedical Engineering, University of Wisconsin—Madison, Madison, Wisconsin 53705, United States^{||}The Cerebrovascular Center and [⊥]Department of Cell Biology, The Cleveland Clinic Foundation, Cleveland, Ohio 44195, United States[¶]Massey Cancer Center, Virginia Commonwealth University, Richmond, Virginia 23298, United States

ABSTRACT: This work utilized polyamidoamine (PAMAM) dendrimer G4.5 as the underlying carrier to construct central nervous system (CNS) therapeutic nanoparticles and explored the buccal mucosa as an alternative absorption site for administration of the dendritic nanoparticles. Opioid peptide DPDPE was chosen as a model CNS drug. It was coupled to PAMAM dendrimer G4.5 with polyethylene glycol (PEG) (i.e., PEG-G4.5-DPDPE) or with PEG and transferrin receptor monoclonal antibody OX26 (i.e., OX26-PEG-G4.5-DPDPE). The therapeutic dendritic nanoparticles labeled with 5-(aminoacetamido) fluorescein (AAF) were studied for transbuccal transport using a vertical Franz diffusion cell system mounted with porcine buccal mucosa. For comparison, AAF-labeled PAMAM dendrimers G3.5 and G4.5 and fluorescein isothiocyanate (FITC)-labeled G3.0 and G4.0 were also tested for transbuccal delivery. The permeability of PEG-G4.5 (AAF)-DPDPE and OX26-PEG-G4.5(AAF)-DPDPE were on the order of 10^{-7} – 10^{-6} cm/s. Coadministration of bile salt sodium glycodeoxycholate (NaGDC) enhanced the permeability of dendritic nanoparticles by multiple folds. Similarly, a multifold increase of permeability of dendritic nanoparticles across the porcine buccal mucosal resulted from the application of mucoadhesive gelatin/PEG semi-interpenetrating network (sIPN). These results indicate that transbuccal delivery is a possible route for administration of CNS therapeutic nanoparticles.

KEYWORDS: Buccal mucosa, central nervous system (CNS), enkephalin, dendrimer, transbuccal delivery, nanomedicine



Nanoparticles have appeared as promising vehicles for efficient delivery of a wide spectrum of central nervous system (CNS) therapeutics (e.g., nucleic acids, proteins, or short peptides) to the brain.^{1–4} Due to the susceptible structures of those bioactive molecules, therapeutic nanoparticles are often administered systemically, most likely via intravenous (i.v.) injection to avoid the first-pass effect and enhance their bioavailability.⁵ Nonetheless, i.v. injection causes poor patient compliance. With the significant increase in the number of CNS drug prescriptions worldwide as predicted, the societal burden of health care services and the risk of cross-contamination of i.v. injection, particularly in developing countries, will be high. Thus, exploring noninvasive and safe administration routes for CNS therapeutic nanoparticles is highly demanded.

Our goal was to develop a modality to administer CNS therapeutic nanoparticles noninvasively. The objective of this work was to apply dendrimers as carriers to deliver CNS drugs and explore the buccal mucosa as an absorption site for administration of CNS therapeutic nanoparticles. The buccal membrane in the oral cavity has a large area, is less affected by saliva, and holds the dosage form for a relatively long time, thus allowing drug molecules to enter the systemic circulation by avoiding first-pass effect. Buccal administration requires much less health care service and offers the advantage of being relatively painless, which

are particular benefits for patients suffering from chronic CNS disorders. Dendrimers are a class of suitable carriers for construction of nanodevices and nanomedicines.^{6,7} They possess a highly branched, nanoscale architecture with very low polydispersity and high functionality.^{6,8,9} The presence of numerous surface groups allows a high drug payload and/or multifunctionality on the dendrimer surface. Several studies have shown that therapeutic molecules can cross cell membranes or biological barriers with the aid of dendrimers.

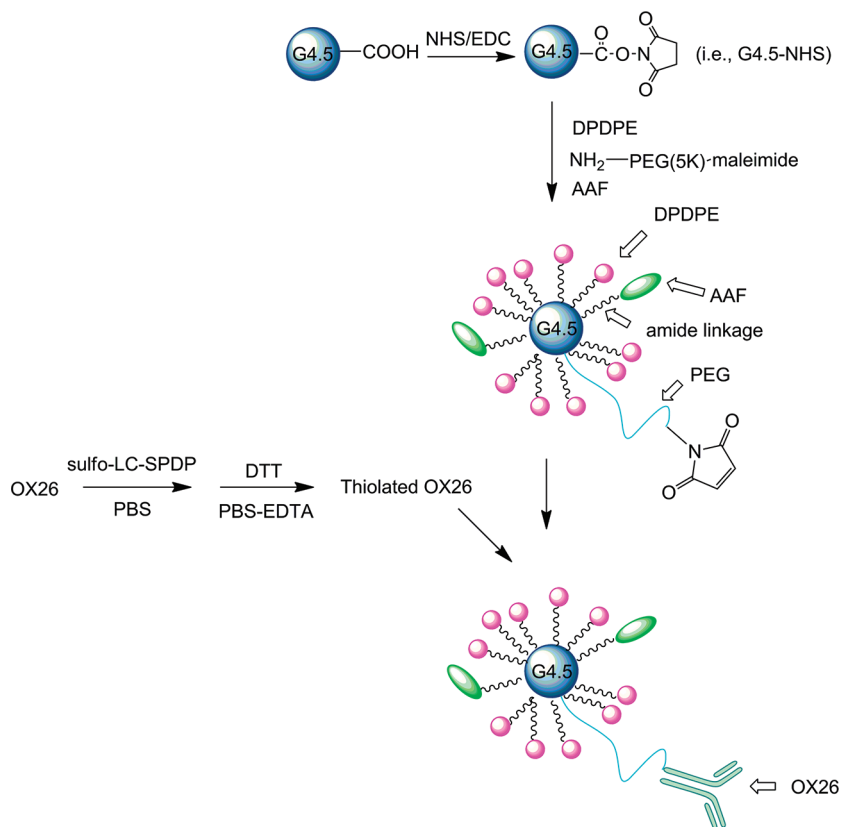
In the present study, DPDPE was chosen as a model drug because it is a well-characterized opioid peptide and has been widely applied to reveal new mechanisms to enhance delivery of peptides into the CNS. Polyamidoamine (PAMAM) dendrimer G4.5 was chosen as the underlying carrier. DPDPE was coupled to the surface of PAMAM dendrimer G4.5 along with polyethylene glycol (PEG). PEG was incorporated into this delivery system to overcome reticuloendothelial system (RES) uptake, reduce immunogenicity and cytotoxicity, and generate favorable pharmacokinetic (e.g., half-lives) and tissue distribution. Additionally, conjugated PEG chains were used as anchoring sites for

Received: August 15, 2011

Accepted: August 29, 2011

Published: August 29, 2011

Scheme 1. Synthesis of PEG-G4.5 (AAF)-DPDPE and OX26-PEG-G4.5 (AAF)-DPDPE Conjugates



coupling of such targeting ligand molecules as OX26, for targeted drug delivery. Porcine buccal mucosa was used as a model to evaluate the permeability of the constructed delivery system, as it is analogous to normal human buccal epithelium in terms of thickness, morphology, structure, and composition.^{10,11} The transbuccal transport of fluorescently labeled PAMAM dendrimers (G3.0, G3.5, G4.0, and G4.5) was investigated for comparison. Bile salt sodium glycodeoxycholate was studied for enhanced transbuccal transport of the therapeutic dendritic nanoparticles. In addition, a mucoadhesive semi-interpenetrating network (sIPN) of gelatin/PEG was applied to formulate buccal adhesive patches for encapsulation and release of the dendritic nanoparticles. The permeability of encapsulated dendritic nanoparticles was determined.

RESULTS AND DISCUSSION

In this work, we developed a CNS drug delivery system based on highly branched, well-defined PAMAM dendrimers. We chose G4.5 as the underlying carrier because it has as many as 128 surface carboxylate groups, high cytocompatibility, and low nonspecific cellular uptake. Since various functional moieties including DPDPE, PEG, fluorescent probe, and targeting ligand OX26 were to be incorporated into the delivery system, we proposed a layer-by-layer assembly strategy to prevent potential cross-reactions. As illustrated in Scheme 1, only complementarily reactive functional groups were made available for coupling reaction in each step: NH_2 and NHS ester in step 1, and maleimide and thiol in step 2. Thiolated OX26 has proven to be efficient in coupling with maleimide-containing polymer.^{12,13}

As thiolation only happens on the carbohydrate part of the Fc portion, the transferrin receptor-recognizing ability of OX26 is preserved.¹⁴

Identification of the maleimide proton peak of PEG (δ 6.69 ppm, peak A), the methylene proton peak of PEG (δ 3.69 ppm, peak B), the methylene proton peak of DPDPE (δ 2.15 ppm, peak C), and multiple proton peaks of G4.5 between 2.19 and 3.47 ppm indicates the success of the synthesis of PEG-G4.5-DPDPE conjugates (Figure 1). Following the methodology described in our previous work,¹⁵ a further calculation was conducted based on the integrals of the corresponding peaks in the spectrum, and it was determined that 97 DPDPE molecules and 3 PEG chains on average were coupled to PAMAM dendrimer G4.5.

To track dendrimers for quantitative assessment of their transbuccal transport, PAMAM dendrimers studied were labeled with fluoresceins. Fluorescein isothiocyanate (FITC) was used to label amine-terminated PAMAM dendrimers G3.0 and G4.0. 5-(Aminoacetamido) fluorescein (AAF) was used to label carboxylate-terminated PAMAM dendrimers G3.5, G4.5, and functionalized PAMAM dendrimer G4.5. PEG-G4.5 (AAF)-DPDPE displayed a measurable size of 73.65 ± 5.96 nm, a nearly 16-fold increase as compared to G4.5-AAF (Table 1). This dramatic size increase was attributed to the conjugation of PEG and DPDPE to the dendrimer and, very likely, the flocculation of individual particles due to entanglement of PEG chains. As a result of surface modification of G4.5, the zeta potential changed from -14.23 ± 0.72 mV for G4.5-AAF to -3.50 ± 0.12 mV for PEG-G4.5(AAF)-DPDPE. Success of coupling OX26 to PEG-G4.5(AAF)-DPDPE was confirmed by Western blotting

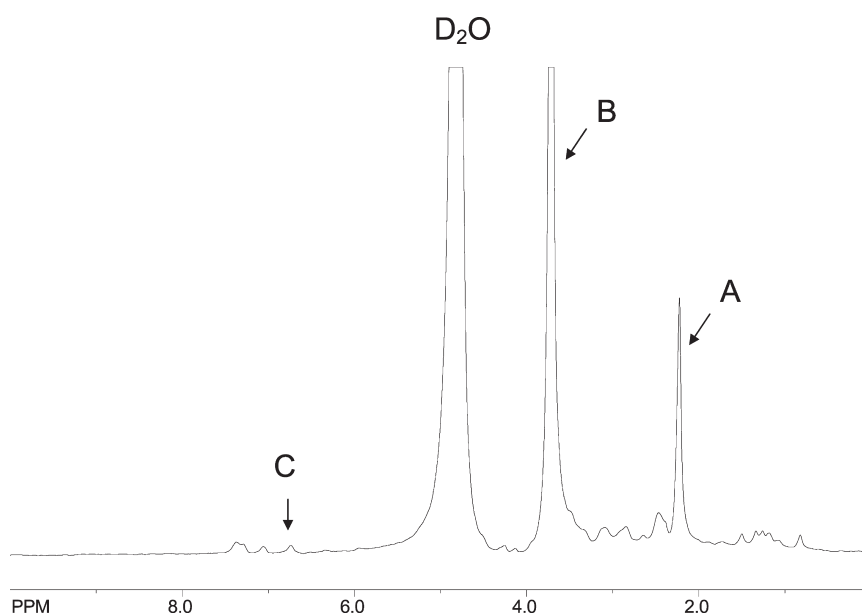


Figure 1. ^1H NMR spectrum of PEG-G4.5-DPDPE conjugates in D_2O .

Table 1. Size and Zeta Potential of the Tested Permeants in pH 7.4 PBS at Room Temperature

permeant	size (nm)	zeta potential (mV)	PDI
G3.0-FITC	3.61 ± 0.71	10.20 ± 0.44	0.427
G3.5-AAF	5.46 ± 0.39	-10.54 ± 0.29	0.487
G4.0-FITC	10.02 ± 0.85	11.99 ± 2.64	0.851
G4.5-AAF	5.54 ± 0.94	-14.23 ± 0.72	0.652
PEG-G4.5 (AAF)-DPDPE	73.65 ± 5.96	-3.50 ± 0.12	0.635
OX26-PEG-G4.5(AAF)-DPDPE	166.20 ± 10.11	-1.5 ± 0.28	0.336
FD-4	77.32 ± 4.68	-4.27 ± 0.59	0.479

(Figure 2) as well as size increase and zeta potential reduction (Table 1). Coupling fluoresceins and other types of moieties to the dendrimer surface resulted in changes in particle size and surface properties. The size and zeta potential of the prepared fluorescently labeled dendrimer derivatives are summarized in Table 1. It is noteworthy that the values of size and zeta potential of dendrimer derivatives reported herein only reflected the surface treatment specified in this work.

The toxicity of PAMAM dendrimers studied in this work was found to be dependent on multiple factors including concentration, generation, surface composition, and incubation period (Figure 3). For a given dendrimer derivative, a shorter period of contact with human dermal fibroblasts had much less toxic effects. For example, the viability of the cells incubated with 2 mg/mL G3.0-FITC increased significantly from 4% to 72% when the incubation period was reduced from 72 to 6 h. As for PEG-G4.5 (AAF)-DPDPE at 2 mg/mL, the cell viability was 68% following 6 h incubation, which was 36% higher than the cell viability following 72 h incubation. Regardless of the length of incubation period, PEG-G4.5 (AAF)-DPDPE at concentrations up to 200 $\mu\text{g}/\text{mL}$ showed good cytocompatibility.

To study transport of PAMAM dendrimers across the porcine buccal mucosa, the permeability of fluorescently labeled

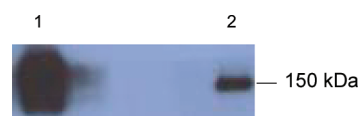


Figure 2. Western blot of OX26-PEG-G4.5 (AAF)-DPDPE (lane 1) and free OX26 (lane 2).

biofunctionalized PAMAM dendrimer G4.5 derivatives, cationic PAMAM dendrimers (G3.0 and G4.0), and anionic PAMAM dendrimers (G3.5 and G4.5) was measured. FD-4 as negative control and benzylamine as positive group were included. As seen from Figure 4, all the cumulative flux curves display a linear range, indicating a steady state transport of the tested permeants via the paracellular route. Permeability was then calculated from the linear range of the cumulative flux curves. Buccal mucosa tissue integrity was confirmed by the low permeability of FD-4, that is, 9.59×10^{-7} cm/s. As expected, benzylamine penetrated the buccal mucosa at a distinctly high influx rate. Its permeability was determined to be 1.01×10^{-5} cm/s.

Hydrophilic molecules can cross the buccal membrane via the paracellular route, which is driven by passive diffusion. G3.0-FITC and G4.0-FITC were found to have significantly higher permeability than G3.5-AAF and G4.5-AAF (Table 2). This result was consistent with a recent study showing that cationic PAMAM dendrimers can gain enhanced transport by causing opening of epithelial tight junctions and toxicity effects.¹⁶ Interestingly noted was that the permeability of PEG-G4.5 (AAF)-DPDPE was 1 order of magnitude higher than that of G4.5-AAF although its size was 12-fold larger. Enhanced transport of PEG-G4.5 (AAF)-DPDPE was presumably attributed to its reduced zeta potential, which, in turn, resulted in enhanced transport of PEG-G4.5 (AAF)-DPDPE across the buccal mucosa tissue. The permeability of OX26-PEG-G4.5(AAF)-DPDPE was lower than that of PEG-G4.5(AAF)-DPDPE by approximately 74%. Nonetheless, the permeabilities of PEG-G4.5 (AAF)-DPDPE and OX26-PEG-G4.5(AAF)-DPDPE were on the order of 10^{-7} – 10^{-6} cm/s

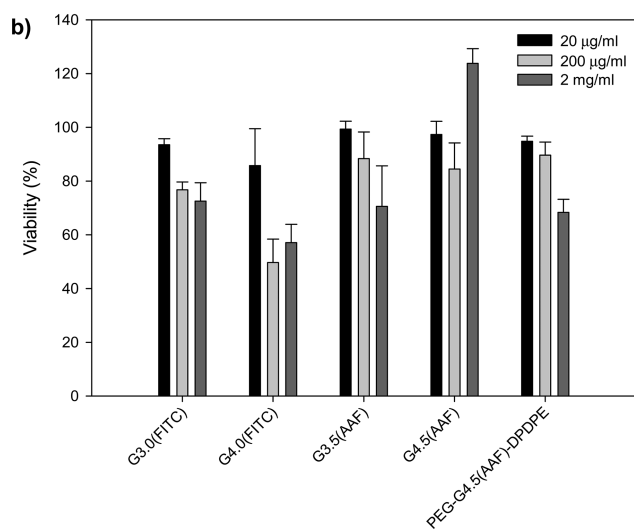
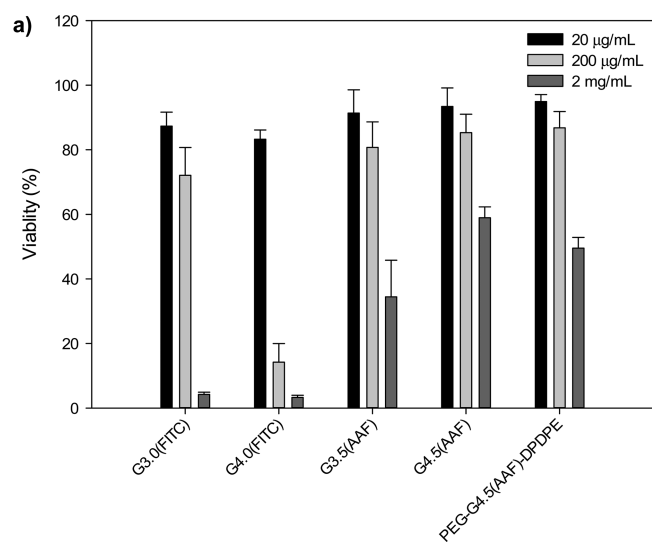


Figure 3. Viability of human dermal fibroblasts incubated with PAMAM dendrimer derivatives for 72 h (a) and 6 h (b).

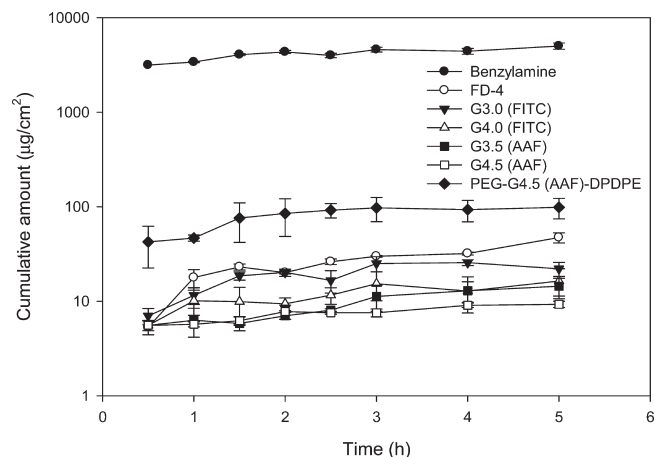


Figure 4. Transport of PAMAM dendrimer nanoparticles across the porcine buccal mucosa.

(Table 2), which was higher than that of G4.5-AAF. The presence of OX26-PEG-G4.5(AAF)-DPDPE permeated through the buccal

Table 2. Permeability of Model Permeants across the Porcine Buccal Mucosa

permeant	permeability (cm/s)
G3.0-FITC	5.45×10^{-6}
G3.5-AAF	2.65×10^{-7}
G4.0-FITC	8.92×10^{-7}
G4.5-AAF	1.06×10^{-7}
PEG-G4.5 (AAF)-DPDPE	3.31×10^{-6}
OX26-PEG-G4.5(AAF)-DPDPE	7.89×10^{-7}
FD-4 ^a	9.59×10^{-7}
Benzylamine ^b	1.01×10^{-5}

^a Negative control. ^b Positive control.

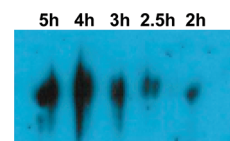


Figure 5. Western blot of OX26-PEG-G4.5 (AAF)-DPDPE permeated through the porcine buccal mucosa at the indicated time points.

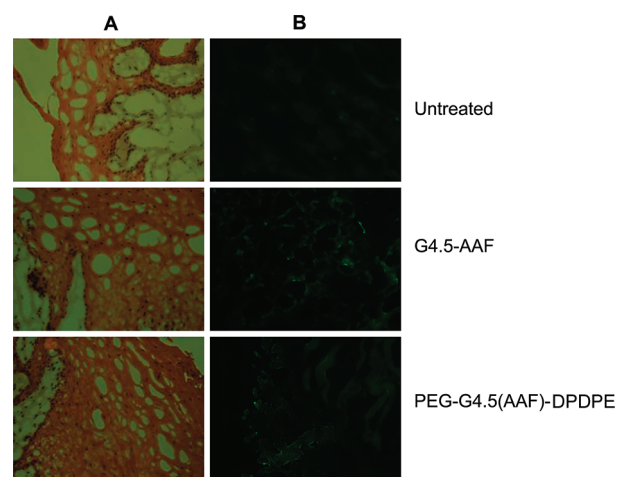


Figure 6. Microscopic examination of the porcine buccal tissues: (A) H&E and (B) fluorescence imaging.

mucosa was further confirmed by Western blotting (Figure 5). According to the microscopic examination of the buccal tissues used in the transport studies of G4.5-AAF and PEG-G4.5 (AAF)-DPDPE, the treated samples did not show any significant difference compared to the untreated tissue (Figure 6, panel A). The fluorescence images (Figure 6, panel B) indicate the presence of G4.5-AAF and PEG-G4.5 (AAF)-DPDPE in the buccal tissues. It was reported that anionic PAMAM dendrimers showed rapid serosal transfer rates in crossing adult rat intestine in vitro and had low tissue deposition.¹⁷ The transport of PAMAM and surface-modified PAMAM across the cell monolayer may follow endocytosis-mediated cellular internalization.¹⁸ Therefore, a mechanistic understanding of transport of dendritic nanoparticles across the buccal mucosa is needed and will be explored in future work.

Flux of nanoparticles across the buccal mucosal membrane can be increased by either elevating nanoparticle concentration

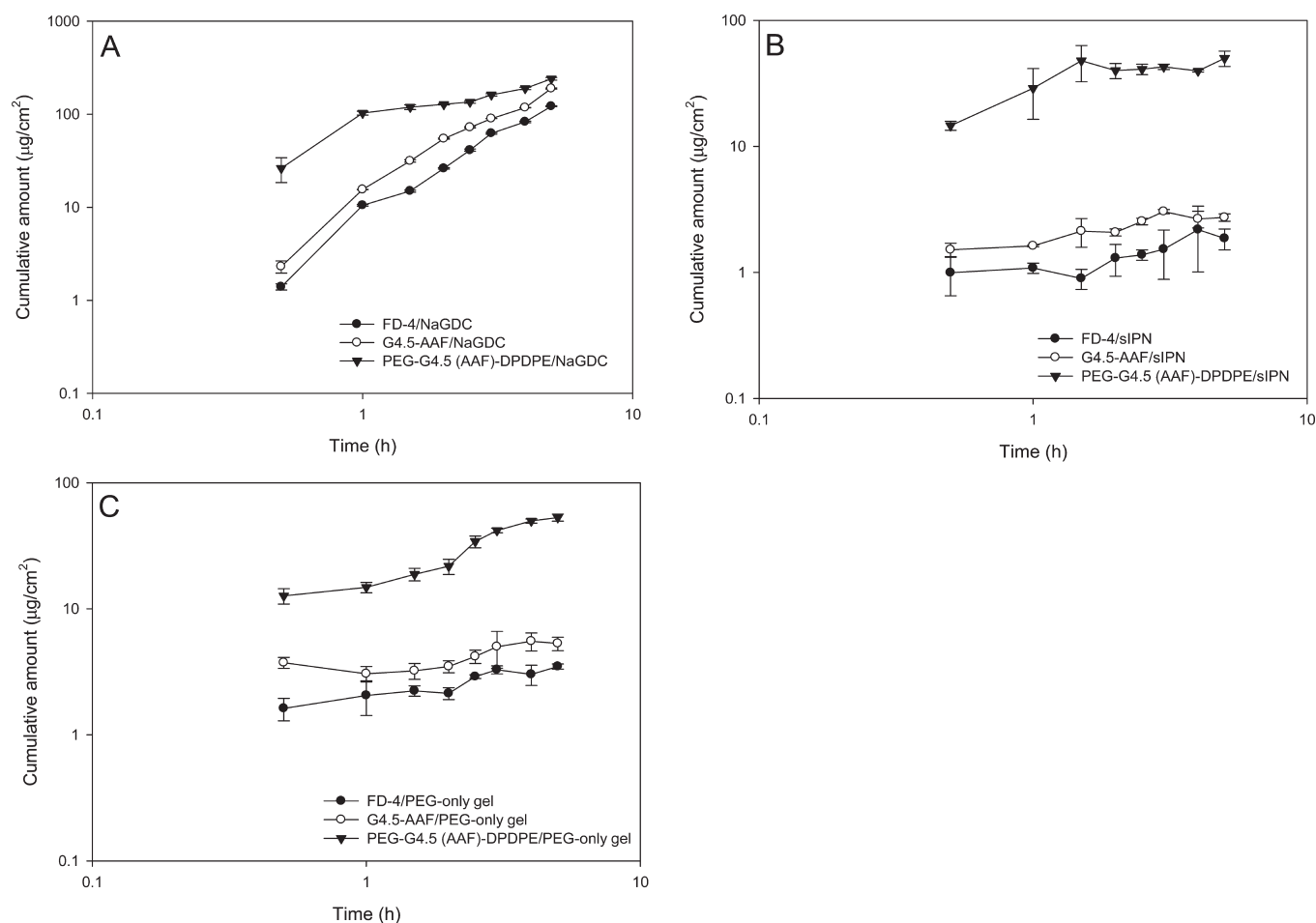


Figure 7. Transport of PAMAM dendrimer nanoparticles across the porcine buccal mucosa with coadministration of sodium glycodeoxycholate (A), from gelatin/PEG sIPN (B), and from PEG-only gel (C).

Table 3. Enhanced Transbuccal Delivery of Dendrimer Nanoparticles by Permeation Enhancer and Hydrogel^a

permeant	condition					
	NaGDC		PEG-only hydrogel		gelatin/PEG sIPN	
	permeability (cm/s)	ER	permeability (cm/s)	ER	permeability (cm/s)	ER
G4.5-AAF	5.03×10^{-6}	47.5	4.25×10^{-7}	4.0	4.25×10^{-7}	4.0
PEG-G4.5 (AAF)-DPDPE	7.71×10^{-6}	2.3	1.06×10^{-5}	3.2	8.92×10^{-6}	2.7
FD-4	4.27×10^{-6}	4.5	4.25×10^{-7}	0.4	2.97×10^{-7}	0.3

^aER: enhancement ratio (permeability obtained under a condition indicated above divided by the permeability of the same permeant reported in Table 2).

gradient for greater fickian diffusion or increasing the permeability of nanoparticles.¹⁹ The latter approach is preferred, as it does not require a high load of therapeutic nanoparticles at the absorption site. Bile salts as penetration enhancer have been applied to enhance permeability of compounds of interest in transbuccal permeation.¹¹ Our work showed that coadministration of NaGDC at 10 mM enhanced the transbuccal permeation of dendrimer nanoparticles (Figure 7A). The permeability enhancement ratios of G4.5-AAF and PEG-G4.5 (AAF)-DPDPE were 47.5 and 2.3, respectively (Table 3). This enhanced transbuccal transport is presumably attributed to the altered intra- and extracellular distribution of permeants by bile salts.¹¹ Therefore,

the low permeability enhancement ratio of PEG-G4.5 (AAF)-DPDPE by NaGDC indicates that the intra- and extracellular distribution of PEG-G4.5 (AAF)-DPDPE might be close to an optimal distribution both intra- and extracellularly. An in-depth examination is needed to gain a clear mechanistic understanding of how structure and composition affect the transport of dendritic nanoparticles across the buccal mucosa. Nonetheless, the use of bile salts is essential for enhanced transbuccal delivery of dendrimers.

Gelatin/PEG sIPN displays good biodegradability, moderate stiffness, and satisfactory tissue adhesiveness.^{20,21} Furthermore, gelatin/PEG sIPN can deliver biomacromolecules such as basic

fibroblast growth factor and release it in a controlled manner.²² Therefore, this mucoadhesive sIPN platform was adopted to formulate buccal patches for delivery of functionalized PAMAM dendrimers. A hydrogel made of PEG only (i.e., PEG-only hydrogel) was used as control. Encapsulated dendrimer nanoparticles were able to permeate through the buccal mucosa at detectable rates as shown in Figure 7B and C. Impressively, permeability of G4.5-AAF and PEG-G4.5 (AAF)-DPDPE was increased significantly after being loaded into sIPN. A 300% increase in permeability for G4.5-AAF and a 170% increase for PEG-G4.5 (AAF)-DPDPE were observed (Table 3). One of the possible factors making mucoadhesive hydrogels increase the permeability of the loaded nanoparticles is that mucoadhesive hydrogels can open up the tight junctions of the epithelium by dehydrating the cells as they swell.²³ Given that the nanoparticles were highly localized on the mucosa surface, the close contact of gel disk and mucosa membrane might facilitate their transbuccal transport as well. The use of PEG-only hydrogel resulted in a slightly higher degree of enhanced transbuccal delivery of G4.5-AAF and PEG-G4.5 (AAF)-DPDPE, which was probably due to the rapid release of those dendritic nanoparticles from the PEG-only hydrogel. However, PEG-only hydrogels do not have mucoadhesiveness and are not a suitable platform for preparation of buccal administration formulations.

In summary, the transbuccal transport of CNS therapeutic dendritic nanoparticles based on PAMAM dendrimer G4.5 was demonstrated. Functionalized PAMAM dendrimer G4.5 displayed a higher permeability than the unmodified counterpart, suggesting that dendrimer surface modification plays an important role determining transbuccal permeation of dendritic nanoparticles. Transbuccal delivery of dendritic nanoparticles was enhanced by permeation enhancer and gelatin/PEG sIPN. Future studies include optimization of a buccal formulation based on gelatin/PEG sIPN loaded with permeation enhancer, further elucidation of the impacts of size and surface properties on the permeability of dendritic nanoparticles, and testing of pharmacokinetics and pharmacodynamics (PK/PD) of therapeutic nanoparticles following buccal administration. Given the high adaptability of PAMAM dendrimers, a wide range of CNS drugs including therapeutic peptides, proteins, and genes will benefit from dendrimer-based delivery and buccal administration.

METHODS

Materials. Ethylene-diamine-core polyamidoamine (PAMAM) dendrimers G3.5 and G4.5 with carboxylate end groups and G3.0 and G4.0 with amine end groups were purchased from Dendritech (Midland, MI). Benzylamine, *N*-hydroxysuccinimide (NHS), 1-ethyl-3-(3-dimethylaminopropyl) carbodiimide hydrochloride (EDC), fluorescein isothiocyanate (FITC), FITC-dextran (FD-4, average molecular weight 3000–5000 Da), and sodium glycodeoxycholate (NaGDC) were obtained from Sigma-Aldrich (St. Louis, MO). 5-(Aminoacetamido) fluorescein (AAF) was purchased from Invitrogen (Carlsbad, CA). [D-Pen 2,5]-Enkephalin (DPDPE) was purchased from AnaSpec (Fremont, CA). Heterobifunctional amine-PEG-maleimide (MW = 3400 Da) was purchased from Creative PEGWorks (Winston Salem, NC). Dialysis membrane (MWCO 14 kDa) was purchased from Spectrum Laboratories (Rancho Dominguez, CA). Mouse monoclonal transferrin receptor antibody OX26 (simply referred to as OX26) was purchased from Abcam (Cambridge, MA). Traut's reagent (i.e., 2-iminothiolane) was purchased from Thermo Scientific (Rockford, IL). Polyvinylidene difluoride (PVDF) membranes (Immobilon-P) were purchased from Millipore (Billerica, MA).

Peroxidase conjugated anti-human secondary antibody was purchased from MP Biomedical (Aurora, OH). All other reagents and solvents used in this work were of analytical grade.

Preparation of PEG-G4.5-DPDPE Conjugates. To synthesize DPDPE-carrying dendrimer conjugates, 13.1 mg of PAMAM G4.5 (0.5 μ mol), obtained upon removal of methanol from the storage solution via rotary evaporation, was dissolved in 2 mL of deionized water and acidified to pH 1.0 with 1 N hydrochloric acid. The acidified G4.5 was evaporated to dryness and then redissolved in 2 mL of a dimethylformamide (DMF)/water solution (80/20 v/v). To the G4.5 solution, 8.9 mg of NHS (77 μ mol) and 15.9 mg of EDC (77 μ mol) were added. After a 14 h reaction while stirring, the resulting NHS-activated G4.5 was dried and redissolved in pH 8.5 sodium bicarbonate solution. PEG- α -amine- ω -maleimide (3.1 mg, 0.9 μ mol) predissolved in pH 8.5 sodium bicarbonate solution was added to the G4.5-NHS solution to initiate a coupling reaction for 3–4 h. Afterward, 150 μ g of AAF (0.36 μ mol) in sodium bicarbonate solution was added slowly to the above reaction mixture and stirred for 2 h. Finally, 1.9 mg DPDPE (2.9 μ mol) was added to the reaction solution for another 3–4 h reaction. The resulting PEG-G4.5-DPDPE conjugates were subjected to dialysis using a dialysis tube with MWCO 14 kDa and then freeze-dried using a Flexi-Dry MP freeze-dryer (FTS, Stone Ridge, NY). The degree of PEGylation and DPDPE loading density were estimated using ¹H NMR spectroscopy.

Preparation of OX26-PEG-G4.5-DPDPE Conjugates. OX26 was coupled to the dendrimer surface via PEG spacer. Briefly, OX26 dissolved in 0.15 M sodium borate buffer/0.1 mM EDTA (pH 8.5) was reacted with Traut's reagent for 1 h at room temperature, where a feed molar ratio of 40:1 for 2-iminothiolane/OX26 was used.^{12,13} PEG-G4.5-DPDPE conjugates were then added to the solution to react with thiolated OX26 overnight with gentle shaking, in which the molar ratio of thiolated OX26 to maleimide was kept at 1:3.¹³ The resulting OX26-PEG-G4.5-DPDPE conjugates were dialyzed for purification.

Fluorescein Labeling of PAMAM Dendrimers. AAF-labeled half-generation PAMAM dendrimers were prepared using NHS/EDC coupling chemistry, similar to coupling of DPDPE to PAMAM dendrimer G4.5. FITC-labeled full generation PAMAM dendrimers G3.0 and G4.0 were prepared following our previous work.²⁴

¹H NMR Spectroscopy. ¹H NMR spectra were obtained on a Varian superconducting Fourier transform NMR spectrometer (Mercury-300). Deuterium oxide (D₂O, 99.9%) was used as the solvent, which has a chemical shift of 4.8 ppm for D₂O residue.

Size and Zeta Potential Measurements. The size and zeta potential of PAMAM dendrimer derivatives in pH 7.4 PBS were measured at room temperature using a Malvern Zetasizer Nano S apparatus (Malvern Instruments, Worcestershire, U.K.).

Fluorometry. Fluorescence spectra were collected on a Cary Eclipse fluorescence spectrophotometer (Varian, Palo Alto, CA) for characterization and quantification of fluorescently labeled dendrimers. FITC-labeled dendrimers and FD-4 were measured at the excitation wavelength of 490 nm and the emission wavelength of 520 nm. AAF-labeled dendrimers were measured at the excitation wavelength of 488 nm and the emission wavelength of 515 nm.

UV–Vis Spectrophotometry. In permeation studies, UV–vis spectrophotometry was applied to quantify benzylamine at the wavelength of 254 nm using a GENESYS 6 UV–vis spectrophotometer.

Western Blotting. OX26-PEG-G4.5-DPDPE was assessed by Western blotting, whereas free OX26 was included as control. They were resolved by SDS-PAGE and then transferred to a polyvinylidene difluoride (PVDF) membrane (Immobilon-P). The membrane was blocked in 5% skimmed milk in TTBS (10 mM Tris-HCl, pH 7.6, 0.5% Tween-20, 150 mM NaCl) for 1 h at room temperature and then incubated in peroxidase conjugated anti-human secondary antibody diluted 1:1000 in blocking buffer overnight at 4 °C. After washing in

TTBS, the antibodies were detected using Western Lightning Enhanced Chemiluminescence (ECL; Perkin-Elmer, Waltham, MA).

Cytotoxicity Studies. Human dermal fibroblasts were seeded at a density of 2×10^4 cells/well in a 6-well cell culture plate. They were maintained in Dulbecco's modified Eagle's medium (DMEM) supplemented with 10% fetal bovine serum (FBS), 100 U mL^{-1} penicillin, and $100 \mu\text{g mL}^{-1}$ streptomycin at 37°C in a humidified atmosphere containing 5% CO_2 in air. The seeded cells were allowed to grow for 24 h and then treated with dendrimer derivatives at various concentrations (0.02 – 2 mg/mL) for 6 or 72 h. Cell viability was then determined using the Trypan blue dye exclusion assay.

In Vitro Permeation Studies. Porcine cheek tissues were obtained from freshly sacrificed pigs (Silver Ridge Slaughter House, Fredericksburg, VA) and transferred to the lab within 2 h. Mucosa tissues were excised and cut into approximately 2 cm^2 and frozen on aluminum foil at -20°C until used. Before permeation studies, frozen specimens were equilibrated in pH 7.4 PBS for 1 h at room temperature to thaw completely. Excesses of connective and adipose tissues were trimmed off with surgical scissors to a thickness of approximately $0.6 \pm 0.1 \text{ mm}$ as determined by using a digital caliper.

Buccal mucosa membrane was mounted on a vertical Franz diffusion cell (PermeGear, Hellertown, PA) with the epithelium facing the donor chamber and the connective tissue facing the receiver chamber. The Franz diffusion cell had a diffusion area of 0.785 cm^2 with a donor chamber volume of 1 mL and a receiver chamber volume of 5 mL. The cell was placed in an incubator, in which temperature was maintained at 37°C and protected against light.

Permeation experiments were carried out using pH 7.4 PBS in the receiver chamber and pH 6.8 PBS in the donor chamber to mimic the in vivo physiological conditions. After an equilibration period of 30 min, PBS in the donor chamber was replaced with 1 mL of PBS containing predissolved dendrimers. In some experiments, NaGDC was coadministered for enhanced transbuccal transport. Its concentration in the donor chamber was kept at 10 mM. To study transbuccal transport of dendrimer nanoparticles loaded into hydrogels, dendrimer-loaded gelatin/PEG sIPN and PEG-only hydrogel disks were prepared as described previously.²⁵ The gel disks of the same size of the permeation surface were placed on top of the mucosa membrane and immersed with 1 mL of pH 6.8 PBS. At a given time point up to 5 h, an aliquot of 0.5 mL from the receiver chamber was collected via syringe and analyzed with fluorometry. FD-4 and benzylamine were included as negative and positive control, respectively.

The permeability coefficient, P , was calculated as follows: $P = (dQ/dt)/AC$, where dQ/dt is the steady-state slope of a cumulative flux curve, C is the loading concentration of a permeant in the donor chamber, and A (0.785 cm^2) is the effective cross-sectional area available for diffusion. Flux ($\mu\text{g/cm}^2/\text{h}$) is determined by $(dQ/dt)/A$. Upon completion of the permeation experiments, the buccal mucosal tissues were processed to get frozen, and hematoxylin and eosin (H&E) stained tissue slices for microscopic examination.

Data Analysis. All bioassays were conducted in triplicate. Collected data were expressed as means \pm SD. One-way ANOVA was performed for statistical analysis. Student's t test was used for pairwise comparison of subgroups. Differences among means were considered statistically significant at a p -value of <0.05 .

AUTHOR INFORMATION

Corresponding Author

*Mailing address: 401 West Main Street, Department of Biomedical Engineering, Virginia Commonwealth University, P.O. Box 843067, Richmond, VA 23284, USA. Telephone: 804-828-5459. Fax: 804-828-4454. E-mail: hyang2@vcu.edu.

Author Contributions

Q.Y. and Y.F. performed the experiments and collected the data. W.J.K. and D.J. designed the experiments. H.Y. conceived and

designed the experiments, analyzed the data and wrote the manuscript.

Funding Sources

This work was supported by NIH R21NS063200 (H.Y.). Frozen and H&E stained OCT embedded porcine buccal mucosal tissue sections were prepared by the VCU Tissue and Data Acquisition and Analysis Core (TDAAC) Facility, supported, in part, with the funding from NIH-NCI Cancer Center Core Support Grant P30 CA016059, as well as through the Department of Pathology, School of Medicine, and Massey Cancer Center of Virginia Commonwealth University.

REFERENCES

- (1) Domb, A., Maniar, M., Bogdanský, S., and Chasin, M. (1991) Drug delivery to the brain using polymers. *Crit. Rev. Ther. Drug Carrier Syst.* 8 (1), 1–17.
- (2) Kreuter, J. (2001) Nanoparticulate systems for brain delivery of drugs. *Adv. Drug Delivery Rev.* 47 (1), 65–81.
- (3) Cornford, E. M., and Hyman, S. (1999) Blood-brain barrier permeability to small and large molecules. *Adv. Drug Delivery Rev.* 36 (2–3), 145–163.
- (4) Yang, H. (2010) Nanoparticle-mediated brain-specific drug delivery, imaging, and diagnosis. *Pharm. Res.* 27 (9), 1759–1771.
- (5) Song, B. W., Vinters, H. V., Wu, D., and Pardridge, W. M. (2002) Enhanced neuroprotective effects of basic fibroblast growth factor in regional brain ischemia after conjugation to a blood-brain barrier delivery vector. *J. Pharmacol. Exp. Ther.* 301 (2), 605–610.
- (6) Tomalia, D. A., Baker, H., Dewald, J., Hall, M., Kallos, G., Martin, S., Roeck, J., Ryder, J., and Smith, P. (1985) A new class of polymers: starburst-dendritic macromolecules. *Polym. J. (Tokyo)* 17 (1), 117–132.
- (7) Tomalia, D. A., Baker, H., Dewald, J., Hall, M., Kallos, G., Martin, S., Roeck, J., Ryder, J., and Smith, P. (1986) Dendritic macromolecules: synthesis of starburst dendrimers. *Macromolecules* 19 (9), 2466–2468.
- (8) Esfand, R., and Tomalia, D. A. (2001) Poly(amidoamine) (PAMAM) dendrimers: from biomimicry to drug delivery and biomedical applications. *Drug Discovery Today* 6 (8), 427–436.
- (9) Newkome, G. R., Yao, Z., Baker, G. R., and Gupta, V. K. (1985) Micelles. Part 1. Cascade molecules: a new approach to micelles. A [27]-arborol. *J. Org. Chem.* 50 (11), 2003–2004.
- (10) Lesch, C. A., Squier, C. A., Cruchley, A., Williams, D. M., and Speight, P. (1989) The permeability of human oral mucosa and skin to water. *J. Dent. Res.* 68 (9), 1345–1349.
- (11) Junginger, H. E., Hoogstraate, J. A., and Verhoef, J. C. (1999) Recent advances in buccal drug delivery and absorption—in vitro and in vivo studies. *J. Controlled Release* 62 (1–2), 149–159.
- (12) Huwyler, J., Wu, D., and Pardridge, W. M. (1996) Brain drug delivery of small molecules using immunoliposomes. *Proc. Natl. Acad. Sci. U.S.A.* 93 (24), 14164–14169.
- (13) Olivier, J. C., Huertas, R., Lee, H. J., Calon, F., and Pardridge, W. M. (2002) Synthesis of pegylated immunonanoparticles. *Pharm. Res.* 19 (8), 1137–1143.
- (14) Pardridge, W. M., Boado, R. J., and Kang, Y. S. (1995) Vector-mediated delivery of a polyamide (“peptide”) nucleic acid analogue through the blood-brain barrier in vivo. *Proc. Natl. Acad. Sci. U.S.A.* 92 (12), 5592–5596.
- (15) Yang, H., and Lopina, S. T. (2006) In vitro enzymatic stability of dendritic peptides. *J. Biomed Mater Res, Part A* 76A (2), 398–407.
- (16) Kitchens, K. M., Kolhatkar, R. B., Swaan, P. W., Eddington, N. D., and Ghandehari, H. (2006) Transport of poly(amidoamine) dendrimers across Caco-2 cell monolayers: Influence of size, charge and fluorescent labeling. *Pharm. Res.* 23 (12), 2818–2826.
- (17) Wiwattanapatapee, R., Carreno-Gomez, B., Malik, N., and Duncan, R. (2000) Anionic PAMAM dendrimers rapidly cross adult rat intestine in vitro: a potential oral delivery system? *Pharm. Res.* 17 (8), 991–998.

- (18) Jevprasesphant, R., Penny, J., Attwood, D., and D'Emanuele, A. (2004) Transport of dendrimer nanocarriers through epithelial cells via the transcellular route. *J. Controlled Release* 97 (2), 259–267.
- (19) Goldberg, M., and Gomez-Orellana, I. (2003) Challenges for the oral delivery of macromolecules. *Nat. Rev. Drug Discovery* 2 (4), 289–295.
- (20) Stevens, K. R., Einerson, N. J., Burmania, J. A., and Kao, W. J. (2002) In vivo biocompatibility of gelatin-based hydrogels and interpenetrating networks. *J. Biomater. Sci., Polym. Ed.* 13 (12), 1353–1366.
- (21) Zilinski, J. L., and Kao, W. J. (2004) Tissue adhesiveness and host response of in situ photopolymerizable interpenetrating networks containing methylprednisolone acetate. *J. Biomed. Mater. Res., Part A* 68 (2), 392–400.
- (22) Burmania, J. A., Stevens, K. R., and Kao, W. J. (2003) Cell interaction with protein-loaded interpenetrating networks containing modified gelatin and poly(ethylene glycol) diacrylate. *Biomaterials* 24 (22), 3921–3930.
- (23) Salamat-Miller, N., Chittchang, M., and Johnston, T. P. (2005) The use of mucoadhesive polymers in buccal drug delivery. *Adv. Drug Delivery Rev.* 57 (11), 1666–1691.
- (24) Yang, H., and Kao, J. W. (2007) Synthesis and characterization of nanoscale dendritic RGD clusters for potential applications in tissue engineering and drug delivery. *Int. J. Nanomed.* 2 (1), 89–99.
- (25) Fu, Y., and Kao, W. J. (2009) Drug release kinetics and transport mechanisms from semi-interpenetrating networks of gelatin and poly(ethylene glycol) diacrylate. *Pharm. Res.* 26 (9), 2115–2124.